Corrosion Behavior and Structure of Plasma Electrolytic Oxidation Coated Aluminum Alloy

Y. Zhang[1,2], W. Fan[1], H.Q. Du[1], Y.W. Zhao[2,]*

[1] School of Mechanical Engineering, Zhejiang Industry Polytechnic College, Shaoxing 312000,China;
[2] Key Lab of E&M, Ministry of Education&Zhejiang Province, Zhejiang University of Technology, Hangzhou 310014, China
E-mail: zyzjipc@126.com

In this study, the plasma electrolytic oxidation (PEO) coatings were formed on aluminum alloy in a cheap and convenient electrolyte. The effect of different current densities, i.e., 5 A/dm^2, 10 A/dm^2, 15 A/dm^2 and 20 A/dm^2 on microstructure and corrosion behavior of coatings was comprehensively studied by scanning electron microscopy (SEM), stereoscopic microscopy, potentiodynamic polarization and electrochemical impedance spectroscopy (EIS) tests, respectively. It was found that the pore density decreased and the pore size increased with the increment of the applied current density. The X-ray diffraction (XRD) results showed that the coatings were only composed of α-Al$_2$O$_3$ and γ-Al$_2$O$_3$. Potentiodynamic polarization test proved that the coating formed under the current density of 10 A/dm^2 showed the best anti-corrosion property. The long time EIS test showed that the coating formed under the current density of 10 A/dm^2 was capable to protect the aluminum alloy substrate after long time of immersion in 0.59 M NaCl solution, which confirmed well with the salt solution immersion test results in 2 M NaCl solution.

1. INTRODUCTION

Aluminum and its alloys have been widely used in aerospace and automotive industry, due to their high specific strength, low density, good formability and non-magnetic properties [1,2]. However, their weakness, the poor corrosion resistance greatly limited the wide application of aluminum alloys, especially like localized damage such as intergranular and pitting corrosion caused by intermetallic constituent particles [3]. Therefore, it is very urgent to improve surface properties and corrosion

resistance of these alloys by surface treatments.

Plasma electrolytic oxidation(PEO), also referred as micro-arc oxidation (MAO), micro-plasma oxidation (MPO) and micro-arc discharge oxidation (MADO) or anode oxidation, has attracted considerable attentions as a surface treatment technology for valve metals (Al, Mg and Ti) and their alloys to form ceramic coatings on the surfaces [4-8]. During the PEO process, the substrate alloy is the anode, the gas layer enshrouding the surface of the alloy consists of oxygen. Specifically, when the dielectric gas layer completely covers the anode surface, numerous sparks appears accompanied the gas bubbles with the PEO treatment continues, provided that the applied voltage higher that the breakdown voltage constantly. Then, a ceramic coating can be formed on the metal surface during the chemical reactions in the plasma environment. Owing to the convenience above, PEO treatment method has been popular in these years.

According to the previous report [9], the PEO process is a multifactor-controlled process. And the properties of PEO coatings can be influenced by many factors, such as electrolytes composition [10-12] and concentration [13], electrical parameters [14], oxidation time [15] and additives [16,17]. To obtain the ideal coatings, many investigations on the factors that influenced coating properties have been carried out in recent years, especially, in the domain of additive. It has demonstrated that the presence of glycerine in the electrolyte composition resulted in not only stabilizing the solution but also achievement of a dense and uniform coating without any cracking. Also, it was effective in enhancement of corrosion resistance of the coating [15]. However, this study was lack of a fully investigation on the effect of current density on the corrosion property of MAO coatings formed in glycerine-containing alkaline electrolyte.

In the present work, plasma electrolytic oxidation of 6063 aluminum alloy was conducted in phosphate-main electrolyte containing glycerine. Corrosion resistance of PEO coatings with the additive formed on 6063 aluminum alloy was studied by potentiodynamic polarization and electrochemical impedance spectroscopy (EIS) test. Further, microstructure and compositions of the coatings were also studied by SEM and XRD.

2. EXPERIMENTATION

2.1. Material and PEO treatment

The substrate material used in this study was 6063 aluminum alloy (wt.%: 0.45~0.90 Mg, 0.35 Fe, 0.2~0.6 Si, 0.10 Cu, 0.10 Mn, 0.10 Cr, 0.10 Zn, 0.10 Ti and balance Al) for PEO treatment. The commercially oblong specimens of the alloy substrate with a size of 30 mm×29 mm×3 mm were grounded by abrasive paper up to # 1800 grits and ultrasonically cleaned in pure ethanol for degreasing, then cleaned by distilled water and dried in hot air. The electrolyte used in this study was an aqueous solution of 30 g/l $(NaPO_3)_6$ + 3 g/l KOH + 8g/l $Na_2B_4O_7$ + 15 g/l glycerin in distilled water. The PEO device was consisted of a pulse 30 kW bipolar power supply (DSM30F) made by Haerbin Disi Numerical Control Equipment Co. Ltd., a stainless steel vessel was used as the electrolytes container, a cooling system and a stirring system to keeping temperature below 303 K in all the cases.

Coatings were produced at the constant current density of 5, 10, 15, 20 A/dm^2 and for 25 min in the electrolyte. After that, they were ultrasonically degreased in ethanol for 20 min, rinsed in distilled water and dried in ambient air.

2.2. Characterization of coatings

The surface and cross-sectional morphology of the coatings were observed using scanning electron microscopy (SEM, ISM-6510). To further analyze the structure of coatings, stereoscopic microscopy (VH-S30B, KEYENCE) was employed to study the surface profile of coatings at the magnification of 5000 ×. Roughness of coatings was measured by a surface profilometer. X-ray diffraction (XRD, Digaku D/max-2500) with Cu Kα radiation was used to study the specific phase composition of the PEO coatings. The 2θ values was of 20° and 80° with a step length of 0.02° and scanning rate of 1°/min. The parameters of X-ray generator were set at 45 kV and 40 mA, respectively. The obtained data was analyzed by Jade 5.0.
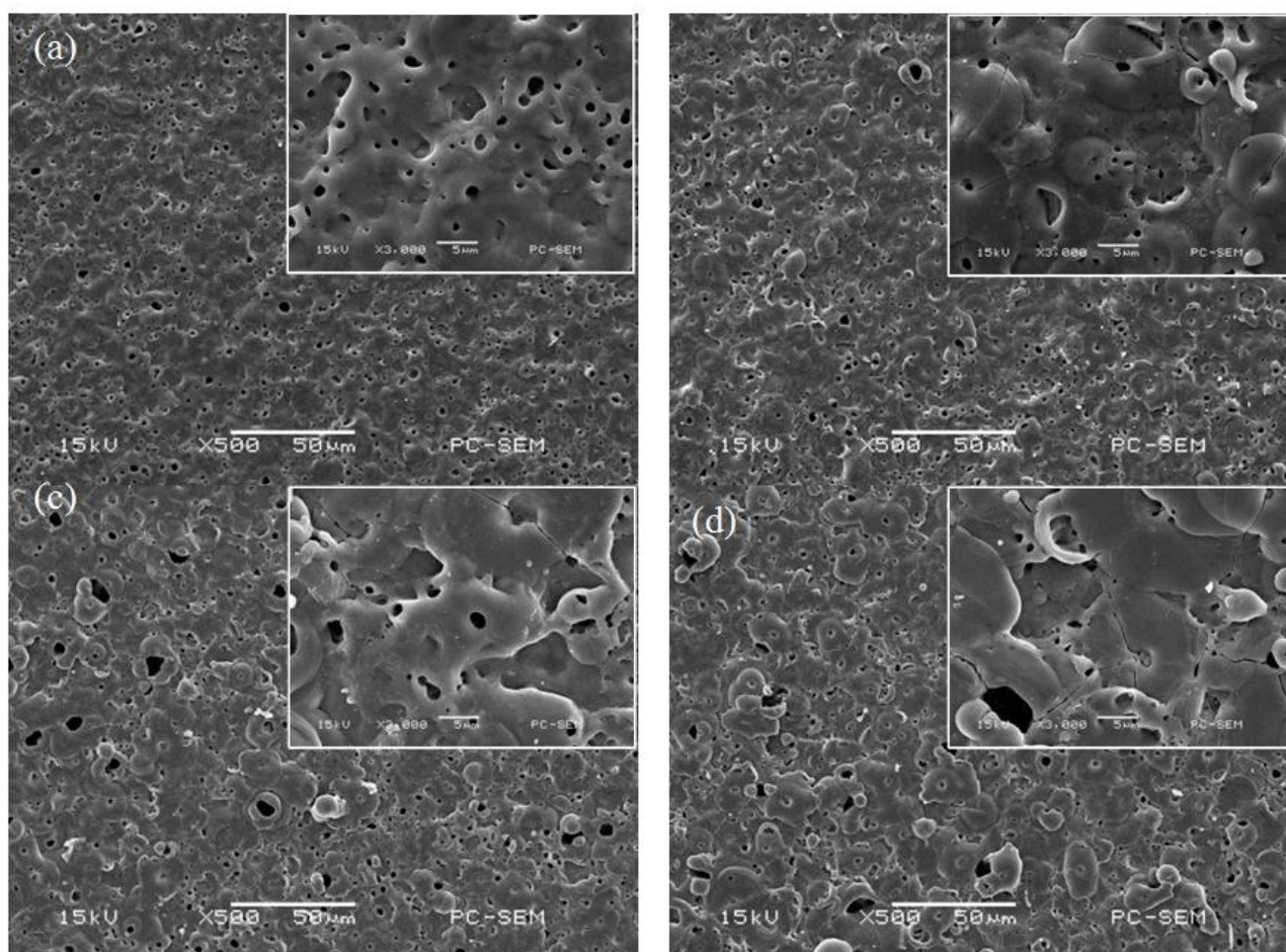
2.3.Potentiodynamic polarization and EIS test

The potentiodynamic polarization and EIS tests were performed in 0.59 M NaCl aqueous solution (pH~7.0) at room temperature (~25 ℃) by means of using an electrochemical system (CS350, Wuhan Corrtest) with the three-electrode-system. The uncoated and PEO coated specimens which were first cut into 1cm^2 and inlaid with resin as the working electrode, a weight-saving platinum electrode as the counter electrode and a saturated calomel electrode (SCE) as the reference electrode. The coated specimen was exposed to the corrosion medium 0.59 M NaCl for 30 min to stabilize its corrosion potential (E_{corr}). Once the open circuit potential (OCP) was nearly stable and fluctuating less than ± 5 mV, the potentiodynamic polarization test was carried out from -1.2 V to -0.4 V (vs. SCE) at a scanning rate of 1 mV/s. The CorShow was the software used to deal with the data of potentiodynamic polarization. As the corrosion status of the electrode system did not significantly influenced by the EIS measurement, it was carried out on the specimen at its corrosion potential. A 10 mV peak-to-peak amplitude potential signal was selected. Frequency range was from 10^5 Hz to 10^{-1} Hz. The coating formed under the current density of 10 A/dm^2 and uncoated 6063 Al alloy were exposed to the 0.59 M NaCl solution for different durations, i.e., 1, 4, 12, 24, 44, 72 h. After EIS experiment, the obtained data were analysed by software (ZSimpWin 3.10) and fitted with the appropriate equivalent circuit models. Under each testing condition, potentiodynamic polarisation curves and EIS measurement were repeated 3-5 times in order to guarantee the reliability and reproducibility. In addition, to directly prove the anti-corrosion properties of coatings, salt solution immersion test was taken to evaluate the corrosion resistance of coatings with 10 days of immersion in 2 M NaCl solution and observed by naked eye.

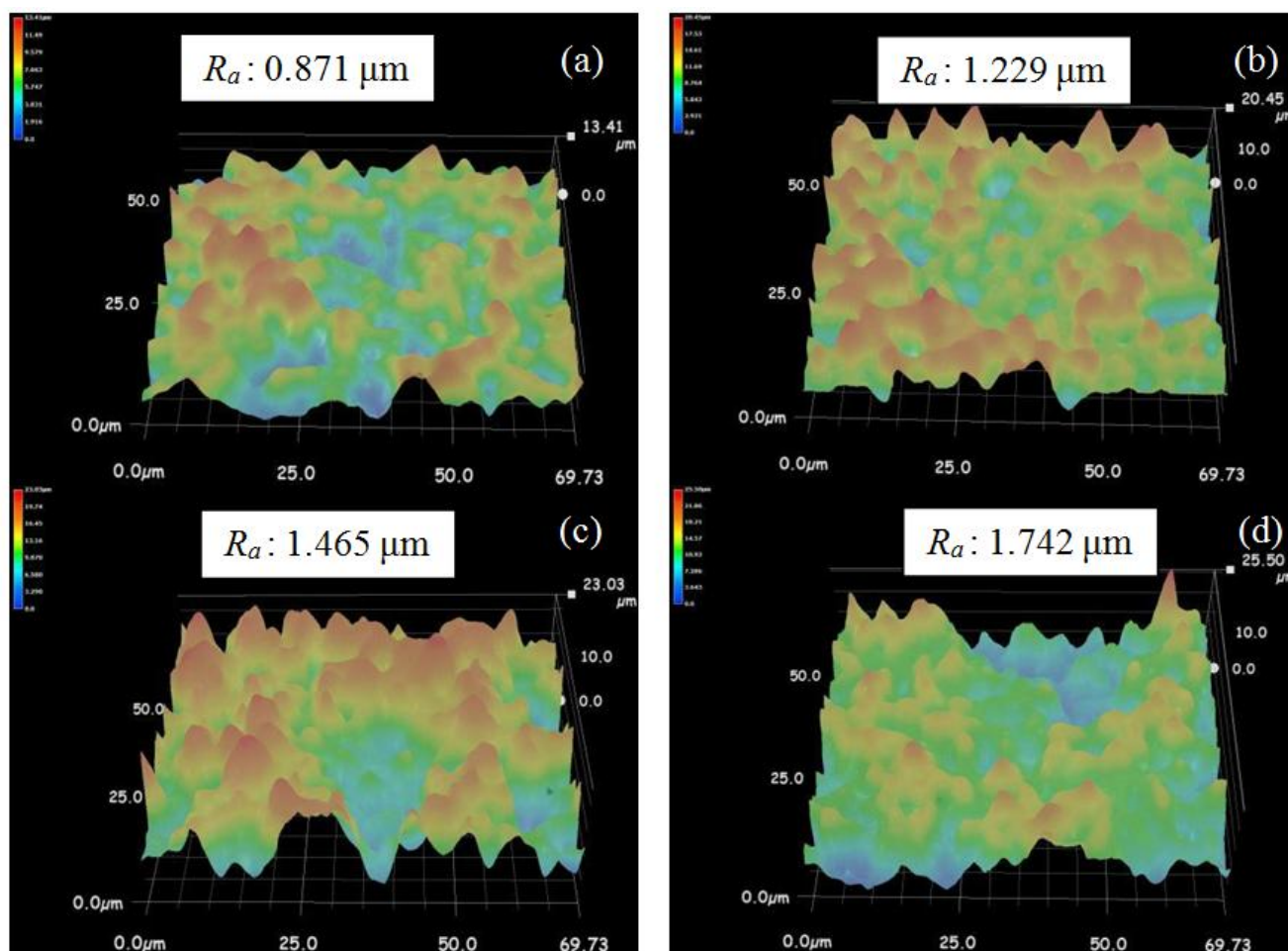## 3. RESULTS AND DISCUSSION

3.1. Morphology

Surface morphology of PEO coatings are presented, as shown in Fig.1. Typical morphology of PEO coatings obtained in phosphate-based electrolyte are presented. All prepared coatings (See Fig.1a-d) were of micropores. Besides, their numbers decreased with the applied current density. However, the size of some micropores increased with increasing the applied current density. Especially, when the current density increased to 15 A/dm^2, some pores with a size of about 4-8 μm appeared. According to Ref.[18], in PEO coatings, the higher voltages are, the larger the pores formed. Especially, when the applied current density increased to 20 A/dm^2, some big microcracks appeared. The appearance of microcracks was probably owing to the thermal stress and high pressure under the high reaction temperature.

Figure 1. Surface morphology of PEO coatings formed under the current density of (a) 5; (b) 10; (c) 15;   (d) 20 A/dm^2 for 25 min.

To better understand the surface structure of coatings, the stereoscopic microscopy was employed to investigate the three dimensional structure of coatings. Fig.2 shows the 3D image of PEO
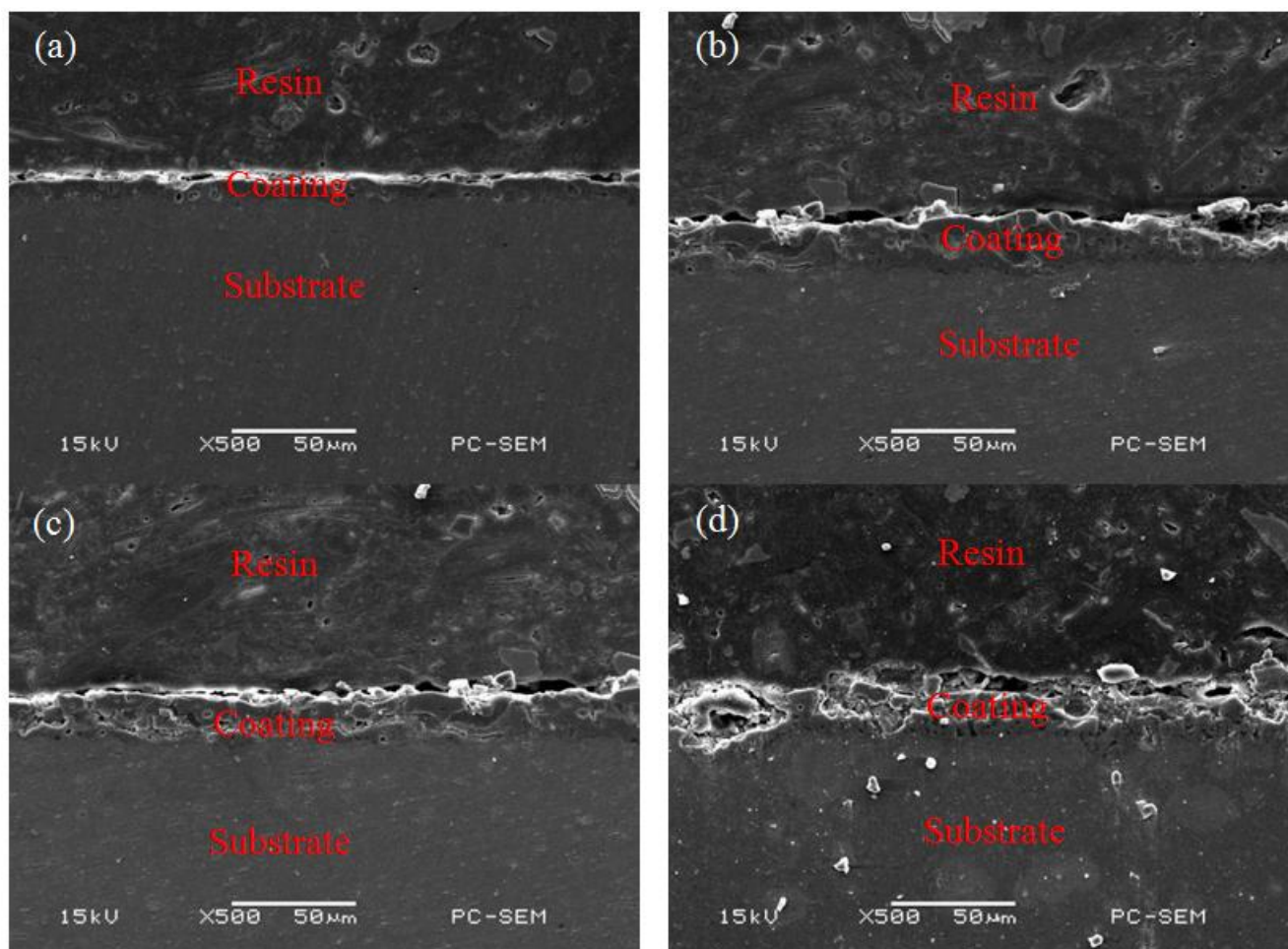
coatings. Generally speaking, in some way, the value in the image on the top-left reflects the surface roughness of coatings. That is, if the coating was of higher value on the image, its roughness will be of higher value either. The bigger the value is, the rougher the coating is. From Fig.2, It is showed that the value on the left-top of the image increased with increasing the applied current density. The PEO coating produced at the current density of 20 A/dm^2 showed the highest mean surface roughness (R_a, ~1.742 μm) among the coatings.

Figure 2. 3D image of PEO coatings formed under the current density of (a) 5; (b) 10; (c) 15; (d) 20 A/dm^2 for 25 min.

The cross-sectional morphology of PEO coatings formed in the applied electrolyte under different current density are shown in Fig.3. The thickness of the coatings first increased when the current density increased to 10 A/dm^2, and then decreased when the current density increased to 15 A/dm^2 and 20 A/dm^2. The average thickness of the coating obtained under the current density of 5, 10, 15, 20 A/dm^2 is about 10.3, 28.6, 23.7, 18.5 μm, respectively. On the other hand, it can be seen that there appears some microcracks on the cross-section of coatings, which indicated that the PEO treatment is very fierce and the coating was destroyed on the minimum extent. Especially, when the current density increased to 15 A/dm^2 and 20 A/dm^2, more microcracks appeared and the coating
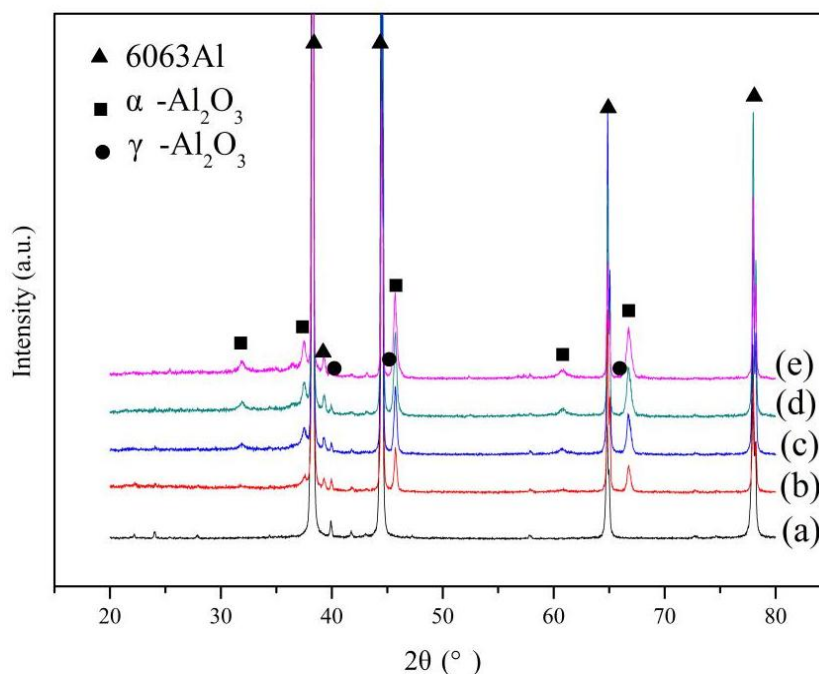
becomes rougher. The coating disposed under the current density of 10 A/dm^2 showed the thickest thickness and was much uniform than the coating obtained under other current densities.

Figure 3. Cross-sectional morphology of PEO coatings formed under the current density of (a) 5; (b) 10; (c) 15; (d) 20 A/dm^2 for 25 min.

3.2. Composition

The phase composition of the PEO coatings formed under the applied electrolyte under different current density investigated by X-ray diffraction (XRD) analysis are shown in Fig.4. The results clearly revealed that the coatings formed in the electrolyte were mainly composed of α-Al$_2$O$_3$ and γ-Al$_2$O$_3$. In the figure, there exists some strong peaks corresponding to the aluminum alloy substrate. So, it should be point out that the strong Al peaks (see Fig.4) corresponding to the aluminum alloy substrate were detected was owing the porosity of the coatings. Which also indicated that the X-rays can easily penetrate through the coatings.
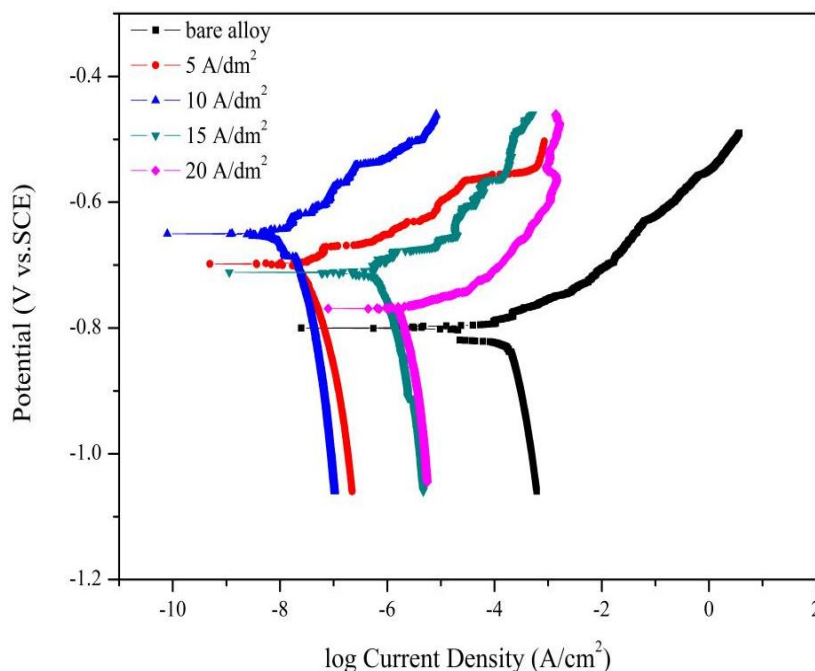
Figure 4. X-ray diffraction patterns of (a) bare alloy and PEO coatings formed under the current density of (b) 5; (c) 10; (d) 15; (e) 20 A/dm^2 for 25 min.

3.3. Corrosion properties

3.3.1. Potentiodynamic polarization test

The potentiodynamic polarization tests of uncoated and PEO coated aluminum alloy were carried out in 0.59 M NaCl after an initial time of 30 min immersion. And the curves are shown in Fig.5. In a typical polarization curve, corrosion potential (E_{corr}) moving to positive direction accompanied by lower current density (i_{corr}) correspond to lower corrosion rate and good corrosion resistance of coatings. The corrosion potential (E_{corr}), current density (i_{corr}) and Tafel slope (β_a) were extracted directly from the potentiodynamic polarization curves by Tafel fit method. The determined parameters related to potentiodynamic polarization curves were listed in Table 1. From Table 1 and Fig.5, it can be seen that the corrosion potential of the coating obtained under the current density of 5 A/dm^2 shifted about 80 mV (vs. SCE) in a positive direction and meanwhile the corrosion current density decreased 1 order of magnitude than uncoated 6063 Al alloy. When the current density increased to 10 A/dm^2, the coating was of the highest corrosion potential and the lowest corrosion current density of -0.653 V and 6.775×10^{-8} A/cm^2. However, when the current density increased to 15 A/dm^2 and 20 A/dm^2, the corrosion potential persistently decreased and the corrosion current density increased with the increasing corrosion current density. Therefore, it can be seen that the coating formed under the current density of 10 A/dm^2 was of the most superior anti-corrosion property among these coatings. The observed i_{corr} value of 6.775×10^{-8} A/cm^2 was comparable to the value of PEO coating obtained in (NaPO$_3$)$_6$+Na$_2$SiO$_3$+ Na$_2$S$_2$O$_3$+NaOH electrolyte [19]. In that electrolyte, the i_{corr} value of the coating was registered at 7.14×10^{-8} A/cm^2, which was a little higher that of the coating

formed in the electrolyte in this study, which indicated that the coating in this study was of better corrosion resistance.

Figure 5. Potentiodynamic polarization curves of uncoated and PEO coated aluminum alloy in 0.59 M NaCl solution. PEO coatings were formed under the current density of 5, 10, 15, 20 A/dm^2.

Table 1. Fitting results of potentiodynamic polarization curves for uncoated aluminum alloy and PEO coatings formed under different current density.
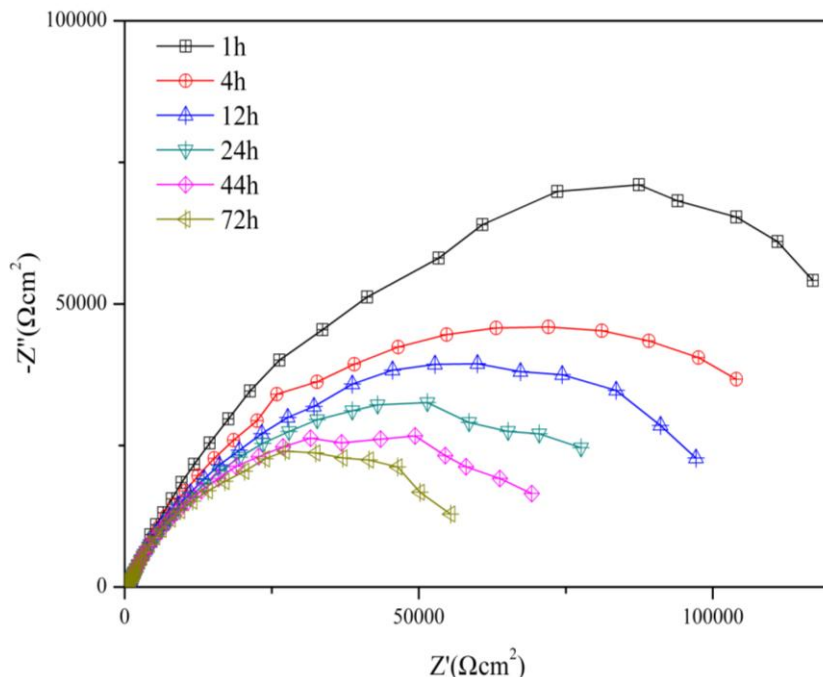
	Bare alloy	5 A/dm^2	10 A/dm^2	15 A/dm^2	20 A/dm^2
E_{corr} (V vs.SCE)	-0.784	-0.706	-0.653	-0.725	-0.763
i_{corr} (A/cm^2)	4.373×10^{-7}	8.947×10^{-8}	6.775×10^{-8}	1.802×10^{-7}	2.513×10^{-7}
β_a (mV/dec)	124	100	91	107	115

3.3.2. EIS analysis and corrosion morphology

According to the result of potentiodynamic polarization test, the coating obtained under the applied current density of 10 A/dm^2 showed the best corrosion resistance. Then, in the following study, the corrosion properties of coating formed under the applied current density of 10 A/dm^2 was investigated by EIS tests additionally.

In order to understand the quantitative corrosion behavior of PEO coating system, the EIS tests were carried out to provide detailed information on the corrosion process at the electrolyte/electrode interface and the property changes of the electrode, which is quite important to understand the corrosion mechanism of coating system [20]. The Nyquist plots for PEO coated and uncoated 6063

aluminum alloy are shown in Fig.6 and Fig.7, respectively. The corresponding simulated data are shown in Table 2 and Table 3.

Figure 6. Nyquist plots of PEO coated aluminum alloy substrate formed under the current density of 10 A/dm^2 immersed in 0.59 M NaCl solution for different times. The fitting equivalent circuits is shown in Fig. 8b and symbols correspond to the experimental values.

Table 2. EIS simulated data of PEO coated aluminum alloy formed under the current density of 10 A/dm^2 immersed in 0.59 M NaCl solution for different times. The fitting equivalent circuits is shown in Fig. 8b and symbols correspond to the experimental values.
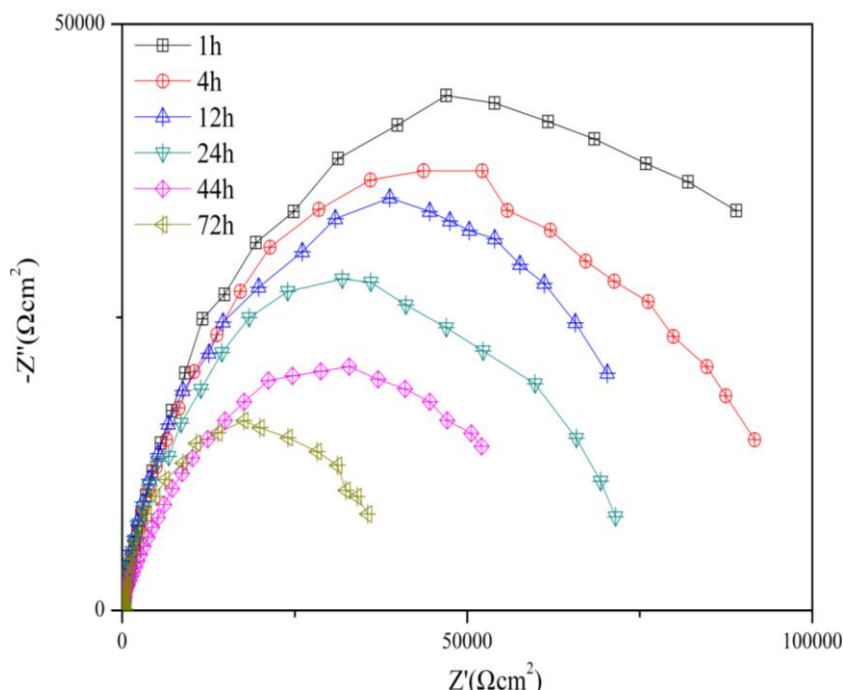
Immersion time	R_s(Ωcm^2)	Q_p(Ω^{-1}s^{n}cm^{-2})	n_p	R_p(kΩcm^2)	Q_b(Ω^{-1}s^{n}cm^{-2})	n_b	R_b(kΩcm^2)
1h	11	1.28×10^{-9}	0.67	28.3	1.38×10^{-9}	0.81	293
4h	16	1.36×10^{-9}	0.84	23.4	1.41×10^{-9}	0.62	258.3
12h	21	1.82×10^{-8}	0.43	21.1	3.15×10^{-8}	0.93	234.5
24h	24	2.64×10^{-8}	0.82	18.4	2.37×10^{-8}	0.73	201.3
44h	27	3.26×10^{-8}	0.55	16.3	2.41×10^{-7}	0.85	192.3
72h	31	2.31×10^{-7}	0.91	14.3	1.73×10^{-7}	0.91	175.8

From Table 2 and 3, it can be seen that the corrosion resistance of bare alloy was significantly improved by PEO treatment. The equivalent circuit model was established in Fig.8 to analyze the EIS results based on a reasonable fitting of the experimental values. The capacitance behavior of coatings and also substrate can be simulated better by constant phase element (CPE) which is represented by symbol Q in this work. The impedance formula for Q is described by the following formula:

$$Z_Q = \frac{1}{Y_0}(j\omega)^{-n} \qquad (1)$$

In this formula, j is an imaginary unit ($j^2 = -1$) and ω is angular frequency ($\omega = 2\pi f$). The coefficient Y_0 or n ($-1 \leq n \leq 1$) is the parameter of CPE.
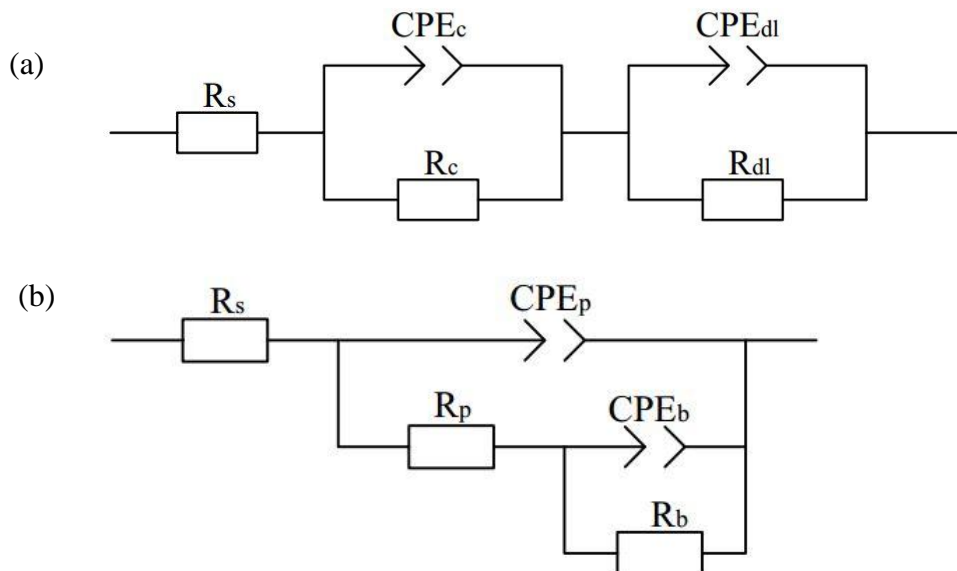
In the presented equivalent circuits in Fig.8, R_s means the solution resistance between specimen and reference electrode, R_p is the resistance of porous layer/coating, paralleled with Q_p (a constant phase element to stand for the dispersion of porous coating/layer capacitance); R_b is donated as the resistance of inner compact layer paralleled with Q_b.

Figure 7. Nyquist plots of uncoated aluminum alloy immersed in 0.59 M NaCl solution for different times. The fitting equivalent circuits is shown in Fig. 8a and symbols correspond to the experimental values.
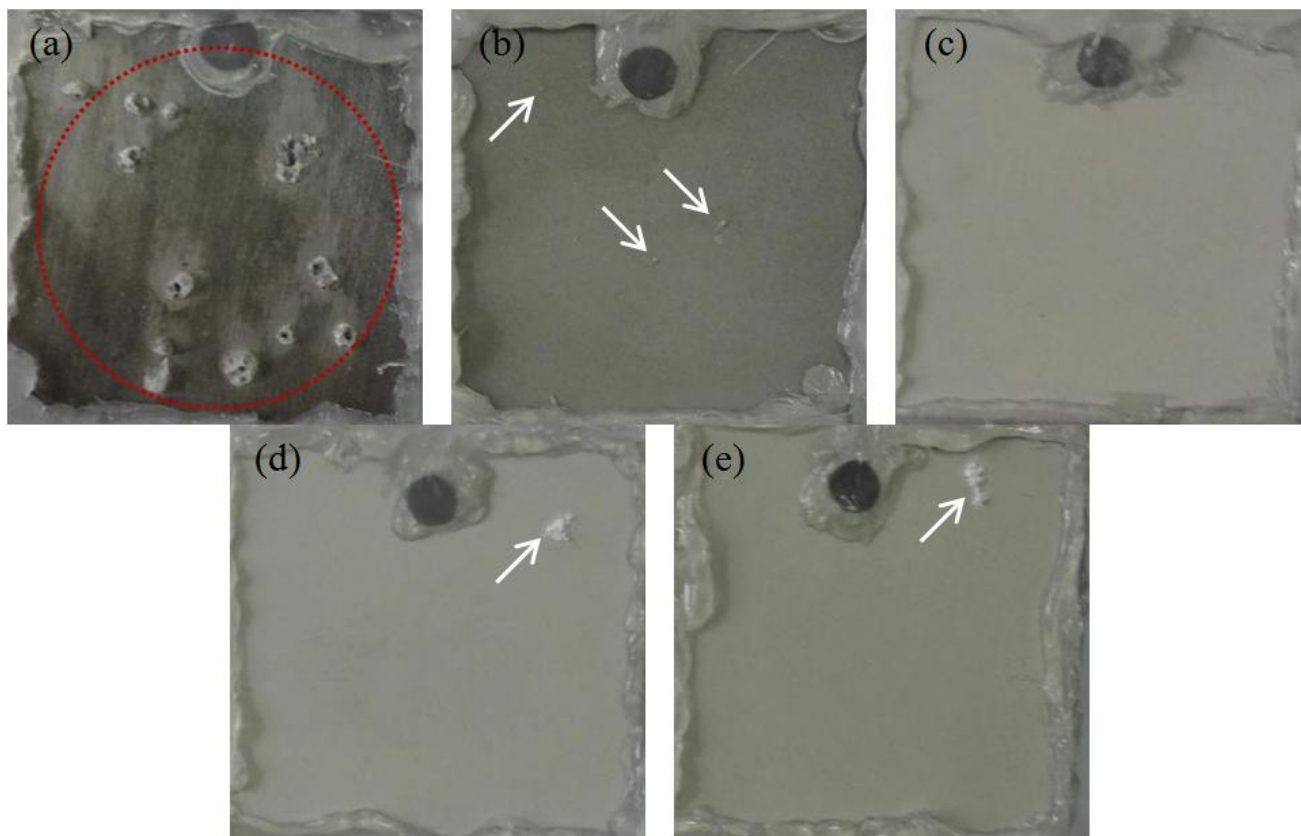
Table 3. EIS simulated data of uncoated aluminum alloy immersed in 0.59 M NaCl solution for different times. The fitting equivalent circuits is shown in Fig. 8a and symbols correspond to the experimental values.

Immersion time	R_s (Ωcm^2)	Q_{dl} ($F\,cm^2$)	n_{dl}	R_{dl} (Ωcm^2)	Q_c ($F\,cm^2$)	n_c	R_c (Ωcm^2)
1h	13	4.23×10^{-4}	0.73	9320	5.26×10^{-5}	0.71	11435
4h	16	4.73×10^{-4}	0.51	8672	4.67×10^{-5}	0.76	9823
12h	21	1.38×10^{-3}	0.65	7634	1.23×10^{-4}	0.81	8567
24h	23	2.24×10^{-3}	0.71	7453	3.26×10^{-4}	0.74	7673
44h	26	4.76×10^{-3}	0.52	7250	5.83×10^{-4}	0.65	7138
72h	31	8.56×10^{-3}	0.67	6250	2.31×10^{-3}	0.82	5267

Figure 8. Corresponding equivalent circuits for fitting the impedance data of (a) uncoated and (b) PEO coated aluminum alloy.

Fig.9 shows the corrosion morphology of uncoated and PEO coated specimen formed under different current densities. The photographs taken of the various samples after salt immersion test in 2 M NaCl aqueous solution for 10 days. The figure revealed that although the surface of the uncoated 6063 aluminum alloy is almost completely covered by corrosion products, whereas the surface of the PEO coatings are much better than the uncoated one after 10 days immersion in 2 M NaCl solution. 3, 0, 1, 1 corrosion pits (shown by white arrows) are developed on the samples anodized in the electrolyte under the current density of 5, 10, 15, 20 A/dm^2, respectively. The corrosion pits on the sample fabricated under the current density of 5 A/dm^2 is very small. However, the corrosion pits on the specimen obtained under the current density of 15 A/dm^2 and 20 A/dm^2 are much bigger. Nevertheless, there is no any evident corrosion pits on the sample obtained under the current density of 10 A/dm^2, which proved that the coating produced under the current density of 10 A/dm^2 was of the most superior corrosion resistance among coatings. This is matched well with the potentiodynamic polarization and EIS tests. In view of the morphology/microstructure (in Fig.1a-d and Fig.3a-d) which linked to the corrosion resistance of PEO coatings, the coating obtained under the current density of 10 A/dm^2 is more smooth than the coating fabricated under the current density of 15 A/dm^2 and 20 A/dm^2. On the other hand, the coating formed under the current density of 10 A/dm^2 showed the thickest thickness. That is, the PEO coating obtained under the current density of 10 A/dm^2 showed the most superior corrosion resistance.

Figure 9. The optical appearance of specimens after salt solution immersion test in 2 M NaCl solution for 10 days: (a) uncoated aluminum alloy and PEO coatings produced under the current density of (b) 5; (c) 10; (d) 15; (e) 20 A/dm^2 for 25 min. The obvious corrosion area are marked by red circles.

4. CONCLUSION

Plasma electrolytic oxidation coatings were formed in phosphate-based electrolyte under different current density with the addition of glycerine. The effect of current density on structure, corrosion properties of PEO coatings were investigated. The conclusion can be drawn as following:

(1) The PEO coating formed under the applied current density of 10 A/dm^2 exhibited relatively better microstructure with less defects. Besides, the coating showed the highest thickness among the coatings. Potentiodynamic polarization test showed that the coating formed under the current density of 10 A/dm^2 showed the best corrosion resistance among these coatings.

(2) EIS tests showed that the PEO coating produced under 10 A/dm^2 was still of ability to protect the aluminum alloy substrate after 72 h immersion in 0.59 M NaCl solution, which was confirmed by 10 days immersion in 2 M NaCl solution.

References

1. L. Wen, Y. Wang, Y. Zhou, J.H. Ouyang, L. Guo, D. Jia, *Corros. Sci.*, 52 (2010) 2687.
2. H.Y. Ding, Z.D. Dai, S.C. Skuiry, D. Hui, *Tribol. Int.*, 43 (2010) 868.
3. G. Bierwagen, R. Brown, D. Battocchi, S. Hayes, *Prog. Org. Coat.*, 68 (2010) 48.
4. H. Fadaee, M. Javidi, *J. Alloys Comp.*, 604 (2014) 36.
5. N. Xiang, R.G. Song, J. Zhao, H. Li, C. Wang, Z.X. Wang, *Trans. Nonferrous Met. Soc. China*, 25(2015) 3323.
6. W. Zhang, B. Tian, K.Q. Du, H.X. Zhang, F.H. Wang, *Int. J. Electrochem. Sci.*, 6 (2011) 5228.
7. T.S. Lim, H.S. Ryu, S.H. Hong, *Corros. Sci.*, 62 (2012) 104.
8. X.L. Zhang, Z.H. Jiang, Z.P. Yao, Z.D. Wu, *Corros. Sci.*, 52 (2010) 3465.
9. Q.B. Li, J. Liang, Q. Wang, Plasma electrolytic oxidation coatings on lightweight metals, in: M. Aliofkhazraei (Ed.), Modern Surface Engineering Treatments, Intech, Rijeka, 2013, pp. 75-99.
10. M. Shokouhfar, C. Dehghanian, A. Baradaran, *Appl. Surf. Sci.*, 257 (2011) 2617.
11. P.Bala Srinivasan, J. Liang, C. Blawert, W. Dietzel, *Corros. Eng. Sci. Technol.*, 46 (2011) 706.
12. Y.C. Jung, K.R. Shin, Y.G. Ko, D.H. Shin, *J. Alloys Comp.*, 586 (2014) S548.
13. Y.L. Cheng, T.W. Qin, L.L. Li, H.M. Wang, Z. Zhang, *Corros. Eng. Sci. Technol.*, 46 (2011) 17.
14. R.O. Hussein, D.O. Northwood, X. Nie, *Surf. Coat. Technol.*, 237 (2013) 357.
15. Z.P. Yao, Y.J. Xu, Y.F. Liu, D.L. Wang, Z.H. Jiang, F.P. Wang, *J. Alloys Comp.*, 509 (2011) 8469.
16. T.S. Lim, H.S. Ryu, S.H. Hong, *Corros. Sci.*, 62 (2012) 104.
17. J. Liang, B.G. Guo, J. Tian, H.W. Liu, J.F. Zhou, T. Xu, *Appl. Surf. Sci.*, 252 (2005) 345.
18. M.K. Arumugam, H.K. Sun, C.J. Hwa, H.P. Young, J.K. Hea, S.S. Kwang, *Ind. Eng. Chem. Res.*, 53 (2014) 9703.
19. D.J. Shen, G.L. Li, C.H. Guo, J. Zou, J.R. Cai, D.L. He, H.J. Ma, F.F. Liu, *Appl. Surf. Sci.*, 287 (2013) 451.
20. C.N. Cao, J.Q. Zhang, An Introduction to Electrochemical Impedance Spectroscopy, Science Press, Beijing, 2002, p. 158 (in Chinese).